PHOTONICS Research

Exceptional points and the ring laser gyroscope

Luke Horstman,[1,3] Ning Hsu,[1,3] James Hendrie,[1] David Smith,[4] and Jean-Claude Diels[1,2,3,*]

[1]School of Optical Science and Engineering, University of New Mexico, Albuquerque, New Mexico 87106, USA
[2]Department of Physics and Astronomy, University of New Mexico, Albuquerque, New Mexico 87131, USA
[3]Center for High Technology Materials, University of New Mexico, Albuquerque, New Mexico 87106, USA
[4]NASA Marshall Space Flight Center, Space Systems Department, Huntsville, Alabama 35812, USA
*Corresponding author: jcdiels@unm.edu

Received 10 June 2019; revised 27 October 2019; accepted 20 December 2019; posted 24 December 2019 (Doc. ID 369521); published 6 February 2020

An equivalence is made between the exceptional points proposed by the field of non-Hermitian quantum mechanics and the dead band observed in laser gyroscopes. The sensitivity enhancement near this exceptional point is plagued by increased uncertainty due to broadening of the beat-note bandwidth. Also, near the dead band the gyroscope response is caused by Rabi intensity oscillations and not solely by a phase modulation. Finally, a distinction is made between conservative and non-conservative coupling.

https://doi.org/10.1364/PRJ.369521

1. INTRODUCTION TO THE LASER GYROSCOPE

Decades ago it was realized that a ring laser could be used for rotation sensing [1]. Two counter-circulating beams form a standing wave fixed in an absolute (i.e., not rotating) frame of reference, which can be used to determine the rate at which a laboratory frame rotates at an angular velocity around it. A small back-scattering can drag the standing wave pattern with the motion of the rotating frame, which is observed as a "dead band" in the response. In order to eliminate this dead band, the mode-locked (ML) laser gyroscope (gyro) was introduced [2].

This bidirectional ML laser is equivalent to a quantum mechanical two-level system perturbed by an electromagnetic field [3]. In this equivalence, the counter-circulating intensities correspond to the diagonal elements of a density matrix, while the off-diagonal elements are associated with the beat signal between the frequency combs issued from the laser. The "transitions" between the two levels are made by the complex coupling between the two intracavity beams. Interest in this quantum mechanical analogy resurfaced with the discovery of the "exceptional points" (EPs) [4].

The laser gyro is a particular example of intracavity phase interferometry (IPI) [5]. In IPI, mode pulling caused by the added phase is exploited to measure many physical quantities, including the Sagnac phase shift in the case of a gyro. As we will see, however, near an EP, the laser signal becomes amplitude modulated, which places limits on EP-enhanced sensing.

2. INTRODUCTION TO EXCEPTIONAL POINTS

It has been shown that non-Hermitian Hamiltonians can result in real and positive spectra if they are parity-time ($\mathcal{PT}$) symmetric [4]. Under certain circumstances, the eigenvalues and eigenvectors of these Hamiltonians coalesce, i.e., one of the eigenmodes becomes fully complex, leading to a situation where the eigenvectors are not orthogonal and therefore no longer span the space. This transitional location in parameter space is known as an EP. The space surrounding this singularity is characterized by a square-root dependence, which is being exploited in optics to enhance the sensitivity of many different systems [6–14], including the laser gyro [15].

The edge of the dead band [1,16–18] of a laser gyro is an example of a non-$\mathcal{PT}$-symmetric EP. This EP arises due to the interplay of the detuning and coupling terms. In contrast, most studies of EP-enhanced sensitivity focus on the $\mathcal{PT}$-symmetric EP that occurs at zero detuning (rotation rate), which relies on the gain difference canceling the purely conservative coupling. However, in real gyroscopes (in particular, cw ones), a non-conservative component of the coupling usually remains.

In this paper it is shown that the non-conservative component of the coupling leads to an amplitude modulation, which in turn causes gain fluctuations that distort the signal. The output pulses are non-sinusoidal, resulting in an accumulation of harmonics in the beat-note spectrum. This broadening increases the uncertainty of the beat-frequency measurement.

Assuming the electric fields within two coupled resonators take the form of $\tilde{E}_{1,2} = \tilde{\mathcal{E}}_{1,2}(t)\exp(-i\omega t)$, and converting to the rotating frame, allows the coupled mode equations describing their complex field amplitudes to be expressed as [19]

$$\begin{aligned}\dot{\tilde{\mathcal{E}}}_1(t) &= \alpha_1\tilde{\mathcal{E}}_1(t) - i\frac{\Delta}{2}\tilde{\mathcal{E}}_1(t) + (s+\tilde{\kappa}_1)\tilde{\mathcal{E}}_2(t),\\ \dot{\tilde{\mathcal{E}}}_2(t) &= \alpha_2\tilde{\mathcal{E}}_2(t) + i\frac{\Delta}{2}\tilde{\mathcal{E}}_2(t) + (s+\tilde{\kappa}_2)\tilde{\mathcal{E}}_1(t),\end{aligned} \tag{1}$$

where the subscripts correspond to the different coupled resonators, $\alpha_{1,2}$ is the saturable (hence, time-dependent) gain/loss coefficient, $\tilde{\kappa}_{1,2}$ is the complex conservative part of the coupling coefficient, s the non-conservative coupling, and Δ is the mode splitting. A detailed explanation of s and $\tilde{\kappa}_{1,2}$ is in Section 3.B.

Postulating the existence of a steady-state solution, one uses the Ansatz

$$\tilde{\mathcal{E}}_{1,2}(t) = A_{1,2}e^{-i\Delta\omega t} \tag{2}$$

for the complex amplitudes where $A_{1,2}$ is a real constant, and then solves the eigenvalue equation

$$\begin{vmatrix} -i\Delta/2 + i\Delta\omega & s + \tilde{\kappa}_1 \\ s + \tilde{\kappa}_2 & i\Delta/2 + i\Delta\omega \end{vmatrix} = 0, \tag{3}$$

where the gain coefficients are both zero at the threshold. In the absence of conservative coupling ($\tilde{\kappa}_1 = \tilde{\kappa}_2 = 0$), the eigenvalues are $\Delta\omega = \pm\sqrt{(\Delta/2)^2 - s^2}$. The EP is then at $\Delta = 2s$. Note that while the Hamiltonian is not $\mathcal{PT}$-symmetric in this case [18], it is a complex symmetric non-Hermitian matrix, which allows real eigenvalues under certain circumstances (i.e., outside of the dead band).

3. DESCRIPTION OF THE LASER GYRO

Applied to a single cavity laser gyro, the two $\pm$ values of $\Delta\omega$ correspond to the frequencies of the counter-propagating electric field amplitudes so that the beat-frequency when the two fields are interfered is $2\Delta\omega$. As Δ is increased (i.e., the gyro is rotated), there is the well-known square-root dependence of the gyro response near its dead band [1,20].

This matches (at first sight) the experimental observations with the ML ring laser sketched in Fig. 1. Two pulses counter-propagate in the ring and meet at the × in the upper branch and again at the bottom of the ring. When the bottom crossing is in air, a linear response without dead band is measured [Fig. 1(a)]. If an interface is introduced at the crossing point, the response includes a dead band as indicated in Fig. 1(b). The dependence indeed follows a square-root curve as in the EP theories, with an infinite differential sensitivity at the edge of the dead band.

However, there is an issue with the steady-state Ansatz of Eq. (2). We can relax this assumption by allowing $A_{1,2}$ to be slowly varying with time (compared to $\Delta\omega$) or by simply solving Eq. (1) numerically. The solutions are then found to be oscillatory close to the EP. Near the EP the solutions are of the form $\tilde{\mathcal{E}}_{1,2}(t) = \tilde{A}_{1,2}(t)\exp[-i\varphi_{1,2}(t)]$, with $\tilde{A}_{1,2}(t) = \cos\Delta\omega t$ and $\varphi_2 - \varphi_1 = \pi/2$. Figure 2 (left) shows the numerical solution close to the EP ($\Delta = 0.101$) for a system assumed to be at equilibrium ($\alpha_{1,2} = 0$), with $s = 0.05$ and $\tilde{\kappa}_1 = \tilde{\kappa}_2 = 0$. As Δ approaches the EP, the polar plot approaches a vertical line. The oscillation is thus an amplitude modulation rather than a frequency modulation at a frequency $\Delta\omega$ that increases with the applied rotation and follows the square-root curve. For large values of Δ, the polar plot (right Fig. 2) shows a perfect circle, indicating that the solution has evolved to the constant amplitude $\tilde{A}_{1,2} = A_{1,2}$ and beat frequency that arises from a pure phase modulation between correlated beams, i.e., $2\Delta\omega = (\varphi_2 - \varphi_1)/t$. The fact that near the EP the beat signal is an amplitude modulation, susceptible to amplitude fluctuations, explains why the steep slope at the foot of the dead band has not found any use in more than 50 years of laser gyro development.

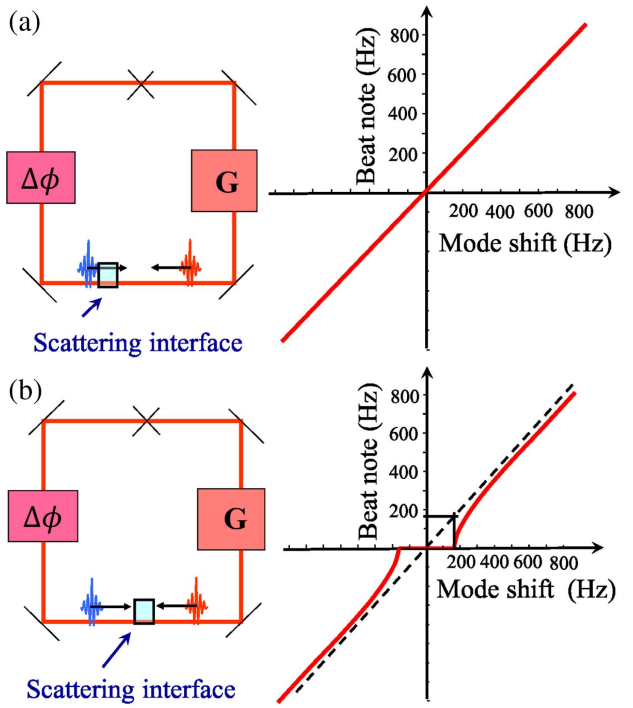

Fig. 1. Sketches of bidirectional ML gyro configurations (left) and their corresponding beat-note responses (right). The × corresponds to a pulse crossing that does not introduce phase coupling. G is the gain, and $\Delta\phi = \Delta/\tau_{rt}$ is the differential round-trip phase shift. Note that the time unit in Eq. (1) has been normalized to τ_{rt}. (a) Linear (i.e., no dead band) response. (b) When a scattering interface is placed at the crossing point, a square-root (i.e., dead band) response is observed (data from Ref. [21]).

A. Presence of Gain Saturation

A real laser system does not have a fixed time-independent gain but a saturable gain. Introduction of a saturable gain in Eq. (1) dramatically changes the behavior close to the EP. The saturable gain coefficient used was $\alpha_{1,2} = \hat{\alpha}_{1,2}/(1 + \beta I_{1,2} + \gamma I_{2,1}) - \alpha_L$, where $\hat{\alpha}_{1,2}$ and α_L are the linear gain and loss coefficients, β and γ are the self and mutual saturation coefficients, respectively, and $I_{1,2}$ are the counter-propagating intensities. Figure 3 (top) shows numerical solutions of

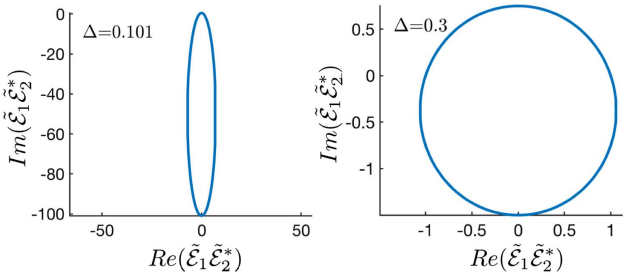

Fig. 2. Polar plots of the imaginary versus real part of the beat field near (left) and far (right) from the EP (dead band). Near the EP the beat note stems from amplitude modulation, while far from the EP it is caused by pure phase modulation.

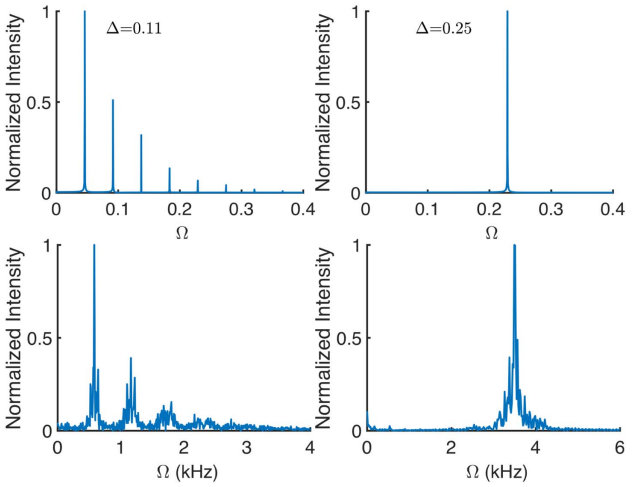

Fig. 3. Beat-signal spectrum from a numerical solution of Eq. (1) (top), and experimentally measured beat-note signal (bottom) showing the clustering of frequency harmonics near the dead band (left) and their absence for larger Δ (right).

Eq. (1) for the parameters $\beta = 1$, $\gamma = 0$, $\hat{\alpha}_{1,2} = 1.1$, $\alpha_L = 1$, $\tilde{\kappa}_1 = \tilde{\kappa}_2 = 0$, and $s = 0.05$.

Experimental data (bottom Fig. 3) was taken using a bidirectional dye-jet ML Ti:sapphire ring laser gyro. Rotation was simulated by applying a voltage to a piece of intracavity lithium niobate that was timed with one of the pulses. At large values of Δ (or lithium niobate voltage), the response is sinusoidal. As Δ is decreased towards the EP, the intensity modulation increases in a nonlinear fashion, and the Fourier spectrum of the beat-note contains an increasing number of harmonics. Similar harmonics as in Figs. 3 and 4 have been observed in Fig. 2 of Ref. [22] for a beat-note spectrum near an EP. A spectrum analyzer with finite bandwidth will measure the center of gravity (COG) of the beat-signal spectrum $\sum_0^\infty \Omega \cdot I(\Omega)^2 / \sum_0^\infty I(\Omega)^2$, which is plotted alongside one of the eigenvalue curves in Fig. 5.

B. Conservative versus Non-Conservative Coupling

To better model experimental situations, the coupling variables in Eq. (1) have been separated into conservative ($\tilde{\kappa}$) and non-conservative (s) terms. The s parameter accounts for any light that is scattered directly into the counter-propagating pulses with a phase that does not follow $\tilde{\kappa}_1 = -\tilde{\kappa}_2^*$. If one face of the scattering window in Fig. 1 is normal to the beam, the coupling between the two beams is fully conservative ($s = 0$), i.e., the total system energy is conserved. A simple proof of this relation is as follows. If the two circulating fields are equal, then the total intensities added to the system by the mutual coupling should be zero, which is proportional to $|1 + \tilde{\kappa}_1 + \tilde{\kappa}_2|^2$, where $\tilde{\kappa}_1$ is the coupling from $\tilde{E}_1$ into $\tilde{E}_2$, and $\tilde{\kappa}_2$ is the exact opposite. For this to be true to first order, $\tilde{\kappa}_1\tilde{\kappa}_2^*$ should be purely imaginary, implying

$$\tilde{\kappa}_1 = -\tilde{\kappa}_2^* \tag{4}$$

or $\tilde{\kappa}_1\tilde{\kappa}_2 = -|\tilde{\kappa}|^2$ [23]. This relation also applies to coupling between fibers and resonators as well as between microresonators [24–26]. For this fully conservative coupling case, the eigenvalues of Eq. (3) are $\Delta\omega = \pm\sqrt{(\Delta/2)^2 + |\tilde{\kappa}|^2}$, which indicates no dead band or EP.

Experiments with a non-normal interface show a dead band of width correlated with the surface quality (scratch-dig), consistent with simulations assuming a non-conservative (nonzero s) scattering [5,21]. Experimental situations likely include coupling contributions from both conservative (due to a non-symmetric interface or evanescent wave coupling) and non-conservative (due to scattering) sources. Including both types of coupling leads to the eigenvalue solutions

$$\Delta\omega = \pm\sqrt{(\Delta/2)^2 + |\tilde{\kappa}|^2 - s(\tilde{\kappa} - \tilde{\kappa}^*) - s^2}. \tag{5}$$

Figure 5 shows numerical solutions to Eq. (1) (with $\alpha_{1,2} = 0$) that display how the gyro beat-note response curve (circles)

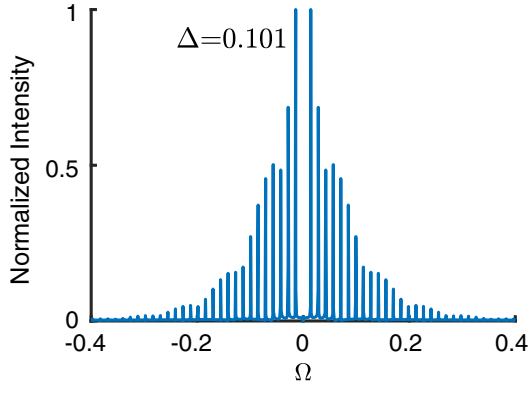

Fig. 4. Beat-signal spectrum from a numerical solution of Eq. (1) showing the clustering of harmonics near the EP (dead band).

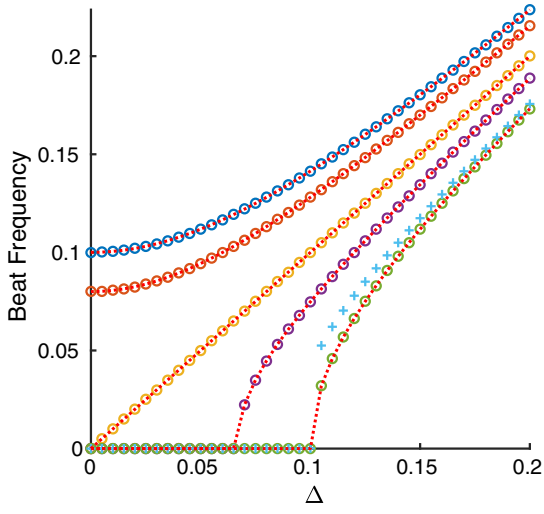

Fig. 5. Gyro beat-note response curve changes with $\tilde{\kappa}$ and s. All large circles are beat frequencies numerically solved from Eq. (1) with $\tilde{\kappa} = 0.05$ and $s = 0$ (blue), $s = 0.03$ (orange), $s = 0.05$ (yellow), and $s = 0.06$ (purple). The green circles are with $\tilde{\kappa} = 0$ and $s = 0.05$. The red-dashed curves correspond to the eigenvalue beat frequency $2\Delta\omega$ determined from Eq. (5). When saturable gain is included, the green circles shift to the positions of the cyan crosses because the COG (rather than the most prevalent peak) of the spectrum must be used. An example of data matching the $\tilde{\kappa} = 0$ case can be found in Ref. [21].

shifts from the fully conservative Hermitian response $\Delta\omega = \pm\sqrt{(\Delta/2)^2 + |\tilde{\kappa}|^2}$ (blue circles) to the fully non-conservative complex symmetric case $\Delta\omega = \pm\sqrt{(\Delta/2)^2 - s^2}$ (green circles) by adjusting the s parameter. Notice that when $|\tilde{\kappa}| > s$ there is not a dead band/EP but a reduction in sensitivity at small Δ. In the experiment sketched in Fig. 1, both s and $\tilde{\kappa}$ can be tuned by adjusting the position and angle of the scattering interface [21]. Note that while $\tilde{\kappa}$ was chosen to be real in this example, the more general case would include a phase factor.

The numerically calculated beat-frequencies plotted in Fig. 5 were found by solving Eq. (1) for $\tilde{\mathcal{E}}_{1,2}(t)$, calculating the intensity when the fields are overlapped in time on a detector $I(t) = |\tilde{\mathcal{E}}_1(t) + \tilde{\mathcal{E}}_2(t)|^2$ and recording the most prevalent peak in the corresponding spectra $I(\Omega) = \mathcal{FT}[I(t)]$. When saturable gain is included, this value would not be experimentally resolvable near the EP. As the EP is approached, the harmonics seen in Fig. 4 will cluster together until they become unresolvable, so the COG of the positive signal would be required, reducing the sensitivity enhancement. This is shown by the cyan crosses in Fig. 5 where saturable gain ($\hat{\alpha}_{1,2} = 1.1$, $\beta = 1$, $\alpha_L = 1$) was included in the purely non-conservative ($\tilde{\kappa} = 0$, $s = 0.05$) curve. Thus, the closer the system is to the EP, the broader and more uncertain the beat-note measurement becomes, and the larger the deviation of the COG from the most prevalent peak is.

C. Gain Difference Exceptional Point

A way to deal with these problems may be to switch to the $\mathcal{PT}$-symmetric EP, which does not suffer from the same broadening into harmonics because, ideally, the temporal oscillations are sinusoidal [18]. Including saturable gain in Eq. (3) leads, with $s = 0$, to an eigenvalue solution of

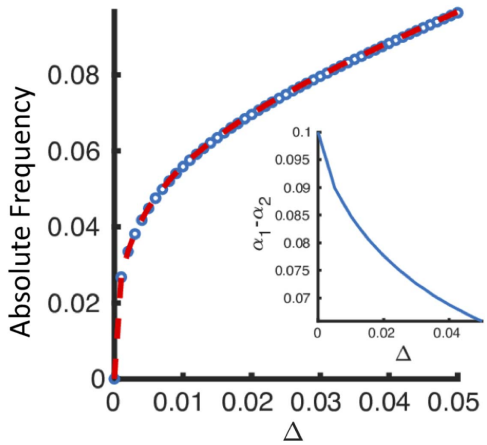

Fig. 6. Numerical solution (blue circles) to Eq. (1) and analytic prediction (red dashes) of Eq. (6) showing an EP at $\Delta = 0$ for $\tilde{\kappa} = 0.05$ with a saturable gain in one resonator, $\hat{\alpha}_1 = 0.051$, $\alpha_L = 0$, $\beta = 1$, $\gamma = 0$, and a constant loss in the other, $\alpha_2 = -|\tilde{\kappa}| = -0.05$. Inset: because the gain difference depends on Δ, it only cancels the coupling exactly at $\Delta = 0$. The time dependence of the fields in polar coordinates is shown in Visualization 1 for $\Delta = 0.01$.

$$\Delta\omega = i\frac{\alpha_1 + \alpha_2}{2} \pm \frac{1}{2}\sqrt{4|\tilde{\kappa}|^2 - [(\alpha_1 - \alpha_2) - i\Delta]^2}. \quad (6)$$

Clearly there is another EP at zero detuning where the positive conservative coupling is offset by the negative gain difference term [15,27]. This EP is $\mathcal{PT}$-symmetric [18], and the response curve is shown in Fig. 6. In this case, the two counter-propagating electric fields have the same frequency (see Visualization 1), which is why Fig. 6 is not a frequency splitting but an absolute frequency that depends on the detuning. This is a result of assuming homogeneous gain saturation. To obtain a frequency splitting, one must use inhomogeneously broadened gain as in Refs. [8,14]. We note that the saturated gain must be different for the two directions to access this EP. In addition, even though it is more sinusoidal, the beat-note at this EP still arises from amplitude modulation. Indeed, we have shown that the use of any EP in a single laser resonator will lead to increased susceptibility to amplitude noise.

Funding. Marshall Space Flight Center (80MSFC19M0042); NASA SBIR (80NSSC19C0505).

REFERENCES AND NOTES

1. F. Aronowitz and R. J. Collins, "Lock-in and intensity-phase interaction in the ring laser," J. Appl. Phys. **41**, 130–141 (1970).
2. M. L. Dennis, J.-C. Diels, and M. Lai, "The femtosecond ring dye laser: a potential new laser gyro," Opt. Lett. **16**, 529–531 (1991).
3. A. Schmitt-Sody, L. Arissian, A. Velten, J.-C. Diels, and D. Smith, "Rabi cycling of two pulses in a mode-locked ring laser cavity with electro-optical control," Phys. Rev. A **78**, 063802 (2008).
4. C. M. Bender and S. Boettcher, "Real spectra in non-Hermitian Hamiltonians having PT symmetry," Phys. Rev. Lett. **80**, 5243–5246 (1998).
5. L. Arissian and J.-C. Diels, "Intracavity phase interferometry: frequency comb sensors inside a laser cavity," Laser Photon. Rev. **8**, 799–826 (2014).
6. R. El-Ganainy, K. G. Makris, M. Khajavikhan, Z. H. Musslimani, S. Rotter, and D. N. Christodoulides, "Non-Hermitian physics and PT symmetry," Nat. Phys. **14**, 11–19 (2018).
7. A. Kodigala, T. Lepetit, and B. Kanté, "Exceptional points in three-dimensional plasmonic nanostructures," Phys. Rev. B **94**, 201103 (2016).
8. W. Chen, Ş. K. Özdemir, G. Zhao, J. Wiersig, and L. Yang, "Exceptional points enhance sensing in an optical microcavity," Nature **548**, 192–196 (2017).
9. J. Wiersig, "Enhancing the sensitivity of frequency and energy splitting detection by using exceptional points: application to microcavity sensors for single-particle detection," Phys. Rev. Lett. **112**, 203901 (2014).
10. H. Hodaei, M.-A. Miri, M. Heinrich, D. N. Christodoulides, and M. Khajavikhan, "Parity-time-symmetric microring lasers," Science **346**, 975–978 (2014).
11. J. Zhu, S. K. Ozdemir, Y.-F. Xiao, L. Li, L. He, D.-R. Chen, and L. Yang, "On-chip single nanoparticle detection and sizing by mode splitting in an ultrahigh-Q microresonator," Nat. Photonics **4**, 46–49 (2009).
12. L. Feng, Z. J. Wong, R.-M. Ma, Y. Wang, and X. Zhang, "Single-mode laser by parity-time symmetry breaking," Science **346**, 972–975 (2014).
13. J. Zhu, Ş. K. Özdemir, L. He, and L. Yang, "Controlled manipulation of mode splitting in an optical microcavity by two Rayleigh scatterers," Opt. Express **18**, 23535–23543 (2010).
14. H. Hodaei, A. Hassan, S. Wittek, H. Garcia-Gracia, R. El-Ganainy, D. Christodoulides, and M. Khajavikhan, "Enhanced sensitivity at higher-order exceptional points," Nature **548**, 187–191 (2017).

15. J. Ren, H. Hodaei, G. Harari, A. U. Hassan, W. Chow, M. Soltani, D. Christodoulides, and M. Khajavikhan, "Ultrasensitive micro-scale parity-time-symmetric ring laser gyroscope," Opt. Lett. **42**, 1556–1559 (2017).
16. R. Adler, "A study of locking phenomena in oscillators," Proc. IRE **34**, 351–357 (1946).
17. J.-C. Diels and I. C. McMichael, "Influence of wave-front-conjugated coupling on the operation of a laser gyro," Opt. Lett. **6**, 219–221 (1981).
18. D. Smith, H. Chang, L. Horstman, and J.-C. Diels, "Parity-time-symmetry-breaking gyroscopes: lasing without gain and subthreshold regimes," Opt. Express (to be published).
19. The equations are written in optics notation so that there is no "i" on the left-hand side. One must use caution when comparing to Schrödinger-like equations and defining hermiticity.
20. F. Aronowitz, "The laser gyro," in *Laser Applications*, M. Ross, ed. (Academic, 1971), pp. 133–200.
21. M. Navarro, O. Chalus, and J.-C. Diels, "Mode-locked ring lasers for backscattering measurement of mirrors," Opt. Lett. **31**, 2864–2866 (2006).
22. Y.-H. Lai, Y.-K. Lu, M.-G. Suh, and K. Vahala, "Observation of exceptional point enhanced Sagnac effect," Nature **576**, 65–69 (2019).
23. This relation depends on the form of the CMEs. If in the form of the Schrödinger equation (with an "i" on the left-hand side), the relation is $\tilde{\kappa}_1 = \tilde{\kappa}_2^*$.
24. J.-C. Diels and W. Rudolph, *Ultrashort Laser Pulse Phenomena*, 2nd ed. (Academic, 2006).
25. A. Yariv, "Universal relations for coupling of optical power between microresonators and dielectric waveguides," Electron. Lett. **36**, 321–322 (2000).
26. R. J. C. Spreeuw, R. C. Neelen, N. J. van Druten, E. R. Eliel, and J. P. Woerdman, "Mode coupling in a He-Ne ring laser with backscattering," Phys. Rev. A **42**, 4315–4324 (1990).
27. H. Wang, S. Assawaworrarit, and S. Fan, "Dynamics for encircling an exceptional point in a nonlinear non-Hermitian system," Opt. Lett. **44**, 638–641 (2019).